

For submission to Dalton Transactions

Redox-active and DNA-binding coordination complexes of clotrimazole

Soledad Betanzos-Lara^{a,+}, Nikola P. Chmel^{b,+}, Matthew T. Zimmerman^c, Lidia R. Barrón-Sosa^a, Claudio Garino^d, Luca Salassa^{e,f}, Alison Rodger^b, Julia Brumaghim^e, Isabel Gracia-Mora^a, and Noráh Barba-Behrens^{a,✉}

^aDepartamento de Química Inorgánica, Facultad de Química, Universidad Nacional Autónoma de México, Ciudad Universitaria, Coyoacán, México, D.F. 04510, Mexico

^bDepartment of Chemistry, University of Warwick CV4 7AL Coventry, England, United Kingdom

^cChemistry Department, Clemson University, Clemson, SC 29634-0973 USA

^dDepartment of Chemistry and NIS Centre of Excellence, University of Turin, Via P. Giuria 7, 10125 Turin, Italy

^e CIC biomaGUNE, Paseo de Miramón 182, 20009 Donostia, Euskadi, Spain

^fKimika Fakultatea, Euskal Herriko Unibertsitatea and Donostia International Physics Center (DIPC), P.K. 1072, 20080 Donostia, Euskadi, Spain

⁺ These two authors are equal first authors

[✉]Corresponding author

SUPPORTING INFORMATION

Table S1

Page S2

Figure S1–S19

Page S3–S22

Because both $[\text{Cu}(\text{clotri})_2\text{Cl}_2]\cdot 5\text{H}_2\text{O}$ (**1**) and $[\text{Cu}(\text{clotri})_2\text{Br}_2]\cdot 5\text{H}_2\text{O}$ (**5**) precipitated from acetonitrile over the course of the electrochemical studies, additional experiments were conducted on both complexes in CH_2Cl_2 , a solvent in which no precipitation occurred. In CH_2Cl_2 , the cyclic voltammogram of **1** shows strong reduction and oxidation waves in the positive region (Figure S20A), consistent with the clotri ligand redox couple ($E_{1/2} = 1.002 \text{ V}$; Table S1). Additional waves for the Cu^{+0} and $\text{Cu}^{2+/+}$ couples are also observed with $E_{1/2}$ potentials of -0.937 and 0.051V, respectively. In comparison, the cyclic voltammogram of **5** shows clotri, $\text{Cu}^{2+/+}$, and Cu^{+0} redox couples (Figure S20B; $E_{1/2}$ values of 1.057, 0.768, and -0.397 V, respectively).

Table S1. Electrochemical potentials (versus NHE) of the Cu²⁺ complexes **1** and **5** determined in dichloromethane.

Compound	<i>E_{p_a}</i> (V)	<i>E_{p_c}</i> (V)	<i>ΔE (V)</i>	<i>E_{1/2} (V)</i>
[Cu(clotri) ₂ Cl ₂]·5H ₂ O (1)	-0.863 ^a , -0.508 ^b , 1.034 ^c	-1.010 ^a , 0.407 ^b , 0.970 ^c	0.147 ^a , 0.915 ^b , 0.064 ^c	-0.937 ^a , -0.051 ^b , 1.002 ^c
[Cu(clotri) ₂ Br ₂]·5H ₂ O (5)	-0.375 ^a , 0.703 ^b , 1.070 ^c	-0.419 ^a , 0.834 ^b , 1.044 ^c	0.044 ^a , 0.131 ^b , 0.026 ^c	-0.397 ^a , 0.768 ^b , 1.057 ^c

^aCu^{+/-} potentials. ^bCu^{2+/+} potentials. ^cClotri ligand potentials.

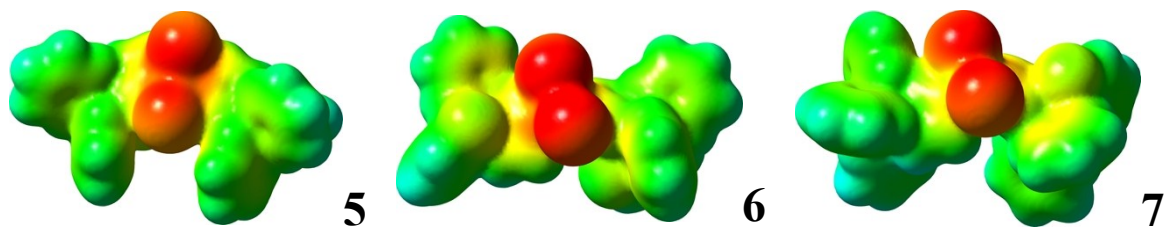


Figure S1. Electrostatic Potential Surfaces (EPS) for complexes **5** - **7** shown in both space and mapped on the electron density (isovalue 0.001) of molecules. The electrostatic potential is represented with a color scale going from red (-0.1 au) to blue (0.1 au).

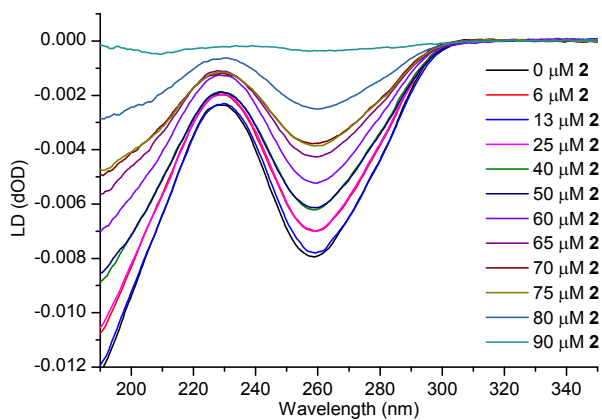


Figure S2. LD spectra of 100 μM DNA with increasing concentration of $[\text{Co}(\text{clotri})_2\text{Cl}_2]$ (**2**).

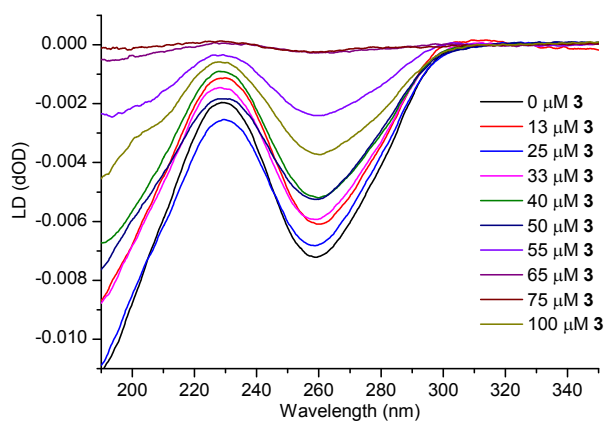


Figure S3. LD spectra of 100 μ M DNA with increasing concentration of $[\text{Zn}(\text{clotri})_2\text{Cl}_2]$ (**3**).

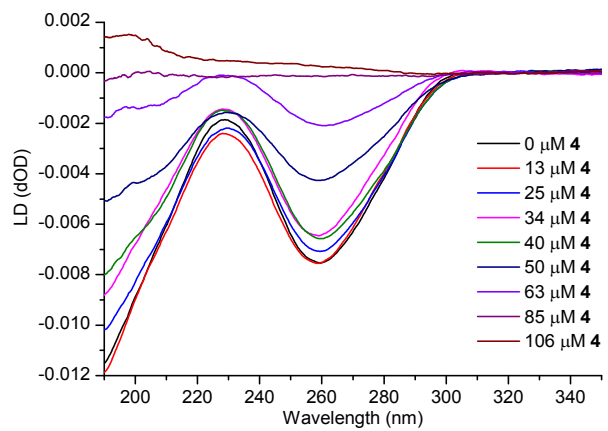


Figure S4. LD spectra of 100 μM DNA with increasing concentration of $[\text{Cu}(\text{clotri})_3\text{NO}_3]\text{NO}_3 \cdot 2\text{H}_2\text{O}$ (**9**).

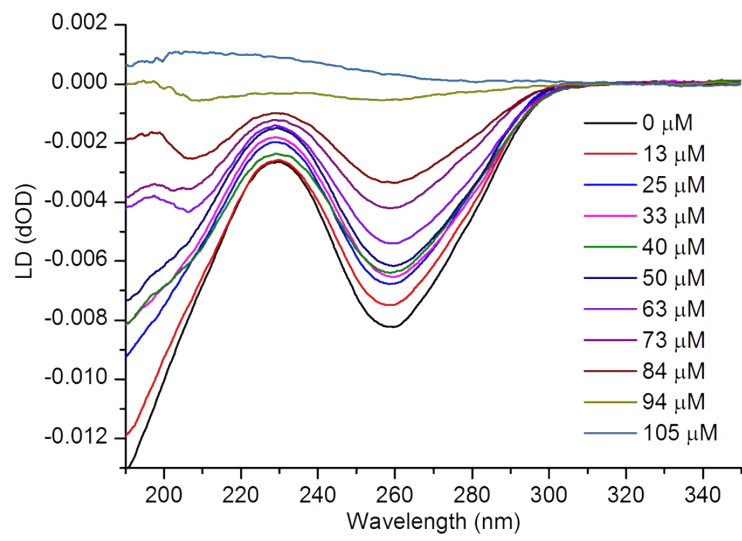


Figure S5. LD spectra of 100 μM DNA with increasing concentration of $[\text{Co}(\text{clotri})_3(\text{NO}_3)_2]$ (10).

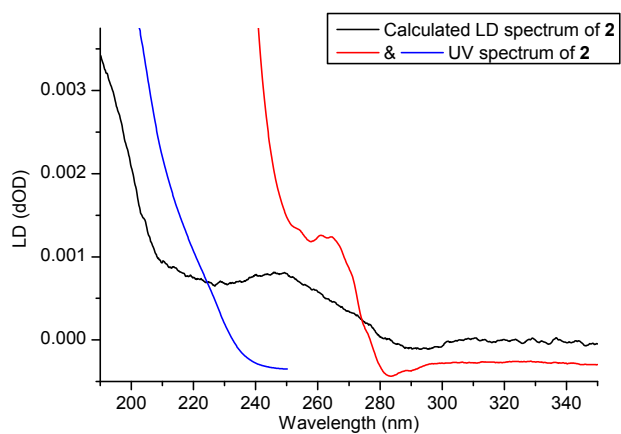


Figure S6. The calculated LD spectrum of $[\text{Co}(\text{clotri})_2\text{Cl}_2]$ (**2**) bound to DNA (black) and an overlaid UV spectrum of $[\text{Co}(\text{clotri})_2\text{Cl}_2]$ (**2**) (red and blue, not to scale).

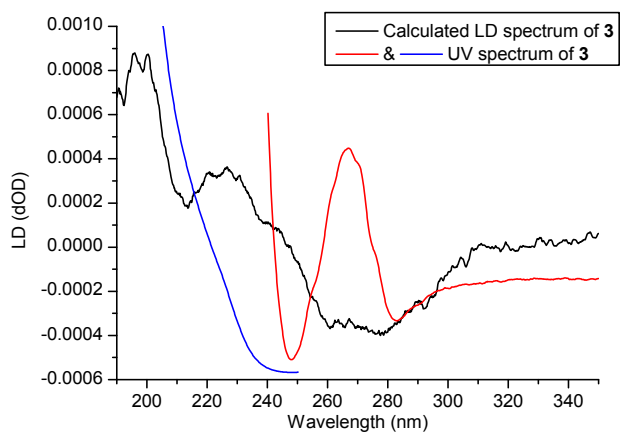


Figure S7. The calculated LD spectrum of $[\text{Zn}(\text{clotri})_2\text{Cl}_2]$ (**3**) bound to DNA (black) and an overlaid UV spectrum of $[\text{Zn}(\text{clotri})_2\text{Cl}_2]$ (**3**) (red and blue, not to scale).

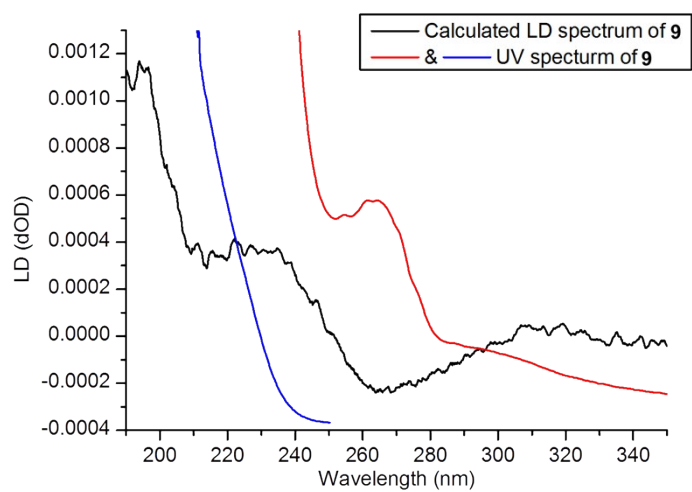


Figure S8. The calculated LD spectrum of $[\text{Cu}(\text{clotri})_3\text{NO}_3]\text{NO}_3$ (**9**) bound to DNA (black) and an overlaid UV spectrum of $[\text{Cu}(\text{clotri})_3\text{NO}_3]\text{NO}_3$ (**9**) (red and blue, not to scale).

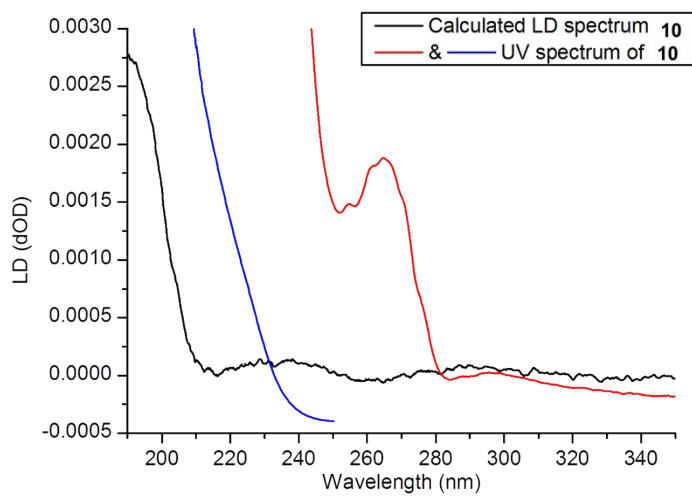


Figure S9. The calculated LD spectrum of $[\text{Co}(\text{clotri})_3(\text{NO}_3)_2]$ (**10**) bound to DNA (black) and an overlaid UV spectrum of $[\text{Co}(\text{clotri})_3(\text{NO}_3)_2]$ (**10**) (red and blue, not to scale).

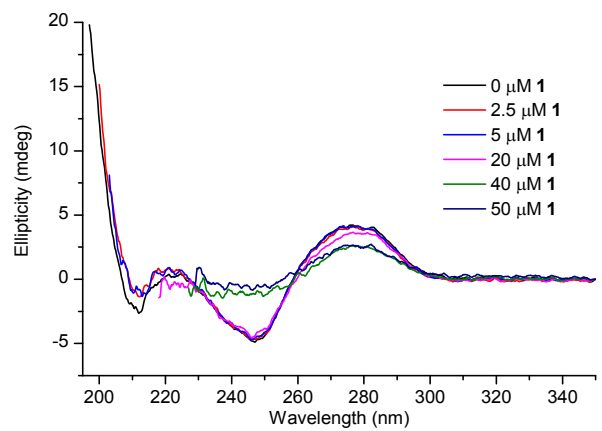


Figure S10. CD spectra of 50 μM DNA with increasing concentrations of $[\text{Cu}(\text{clotri})_2\text{Cl}_2]$ (1).

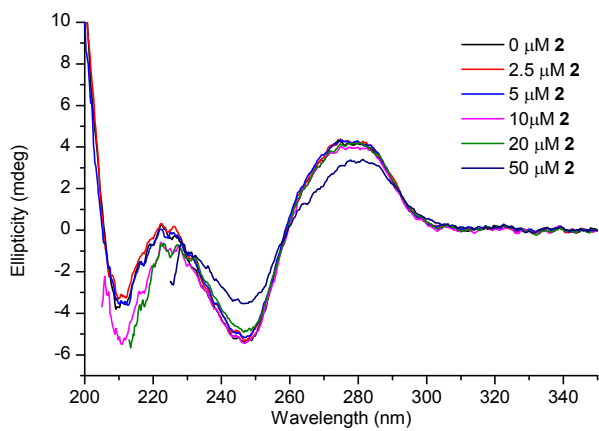


Figure S11. CD spectra of 50 μ M DNA with increasing concentrations of $[\text{Co}(\text{clotri})_2\text{Cl}_2]$ (**2**).

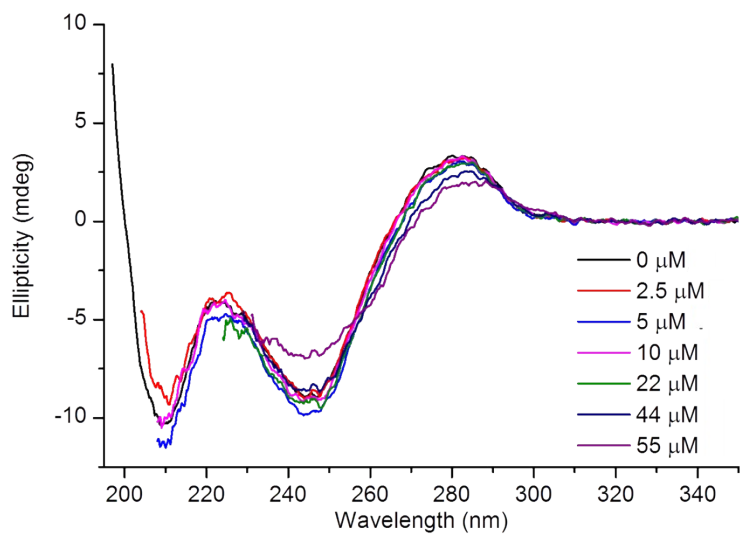


Figure S12. CD spectra of 50 μM DNA with increasing concentrations of $[\text{Cu}(\text{clotri})_3\text{NO}_3]\text{NO}_3$ (**9**).

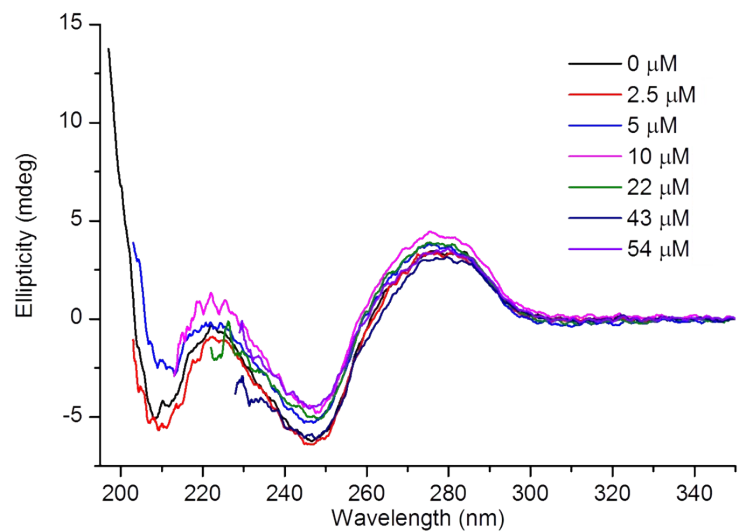


Figure S13. CD spectra of 50 μ M DNA with increasing concentrations of $[\text{Co}(\text{clotri})_3(\text{NO}_3)_2]$ (10).

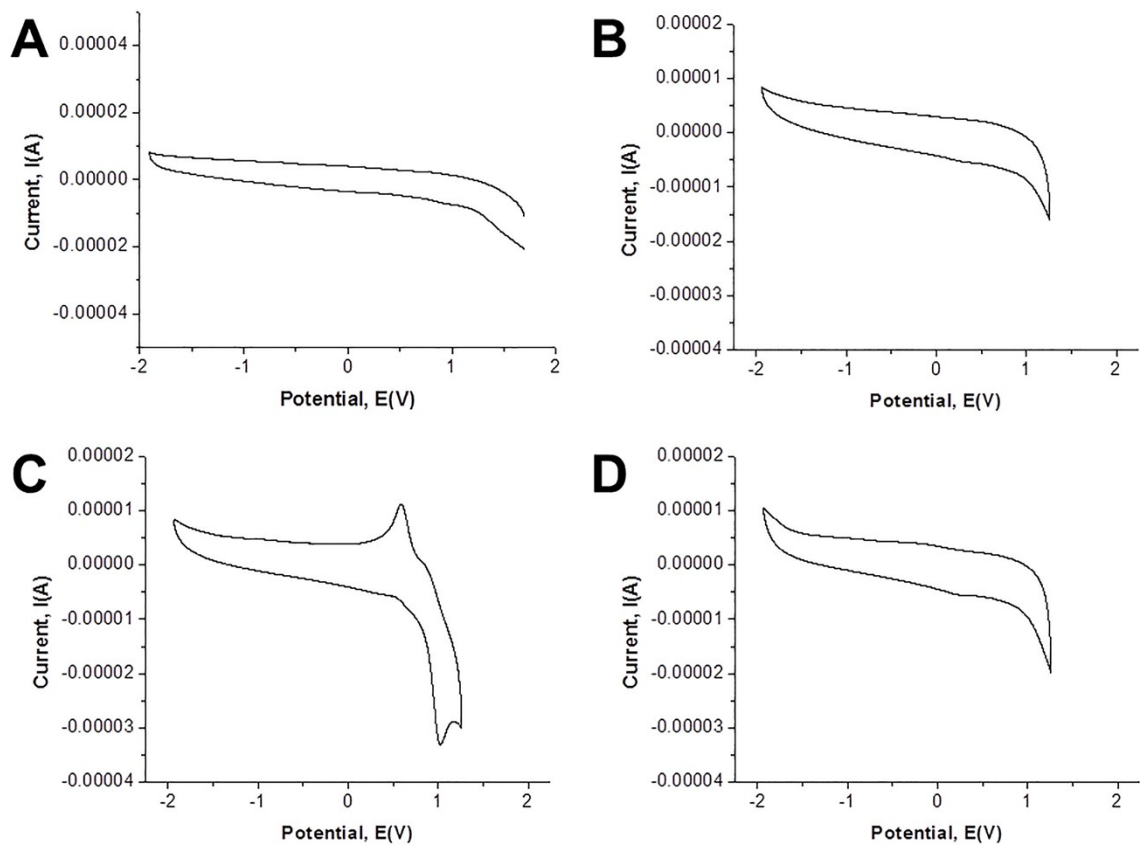


Figure S14. Cyclic voltammograms vs. NHE for A) clotrimazole, B) $[\text{Zn}(\text{clotri})_2\text{Cl}_2]$ (1 mM), C) $[\text{Zn}(\text{clotri})_2\text{Br}_2]$ (1 mM), and D) $[\text{Zn}(\text{clotri})_3\text{NO}_3]\text{NO}_3 \cdot 5\text{H}_2\text{O}$ (1 mM) in acetonitrile with 0.1 M TBAPF₆ as the supporting electrolyte.

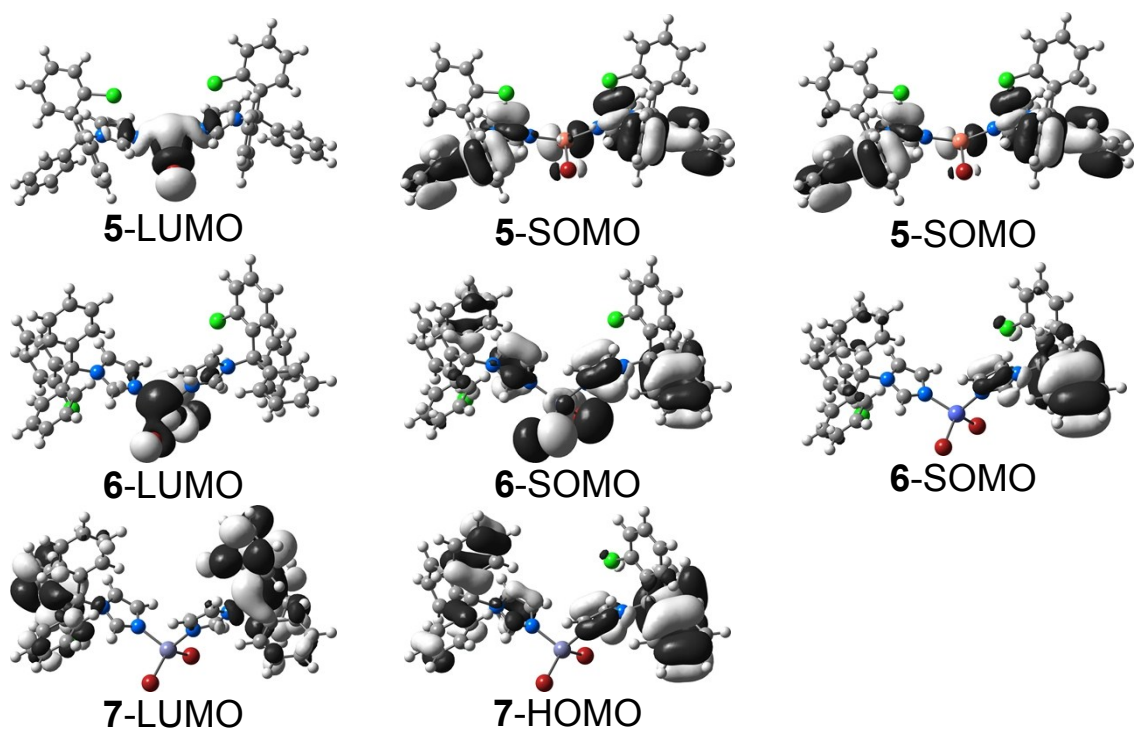


Figure S15. Calculated frontier molecular orbitals for complexes **5–7**. HOMO = highest occupied molecular orbital, SOMO = singly occupied molecular orbital, LUMO = lowest unoccupied molecular orbital.

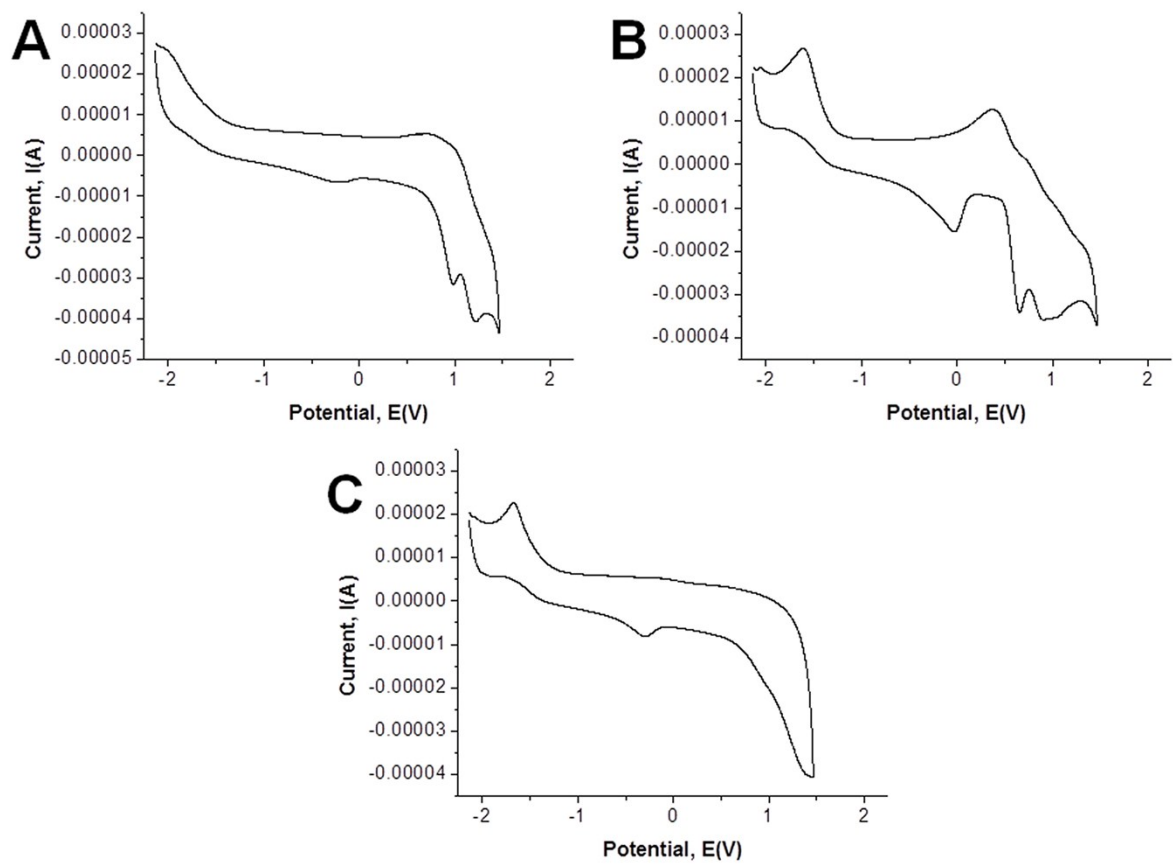


Figure S16. Cyclic voltammograms vs. NHE for A) $[\text{Co}(\text{clotri})_2\text{Cl}_2]$ (**2**) (1 mM), B) $[\text{Co}(\text{clotri})_2\text{Br}_2]$ (**6**) (1 mM), and C) $[\text{Co}(\text{clotri})_3(\text{NO}_3)_2]$ (**10**) (1 mM) in acetonitrile with 0.1 M TBAPF₆ as the supporting electrolyte.

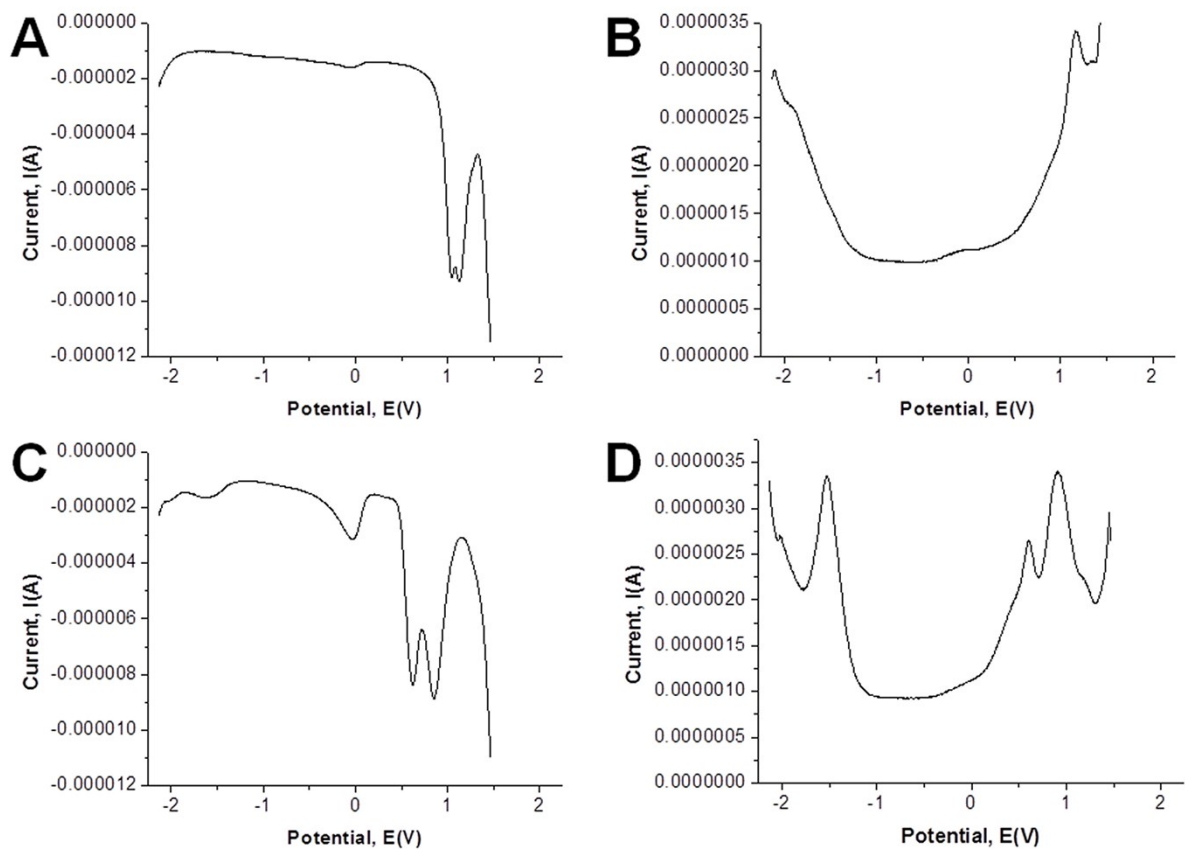


Figure S17. Differential pulse voltammograms vs NHE (A) $[\text{Co}(\text{clotri})_2\text{Cl}_2]$ (2) positive scan, (B) $[\text{Co}(\text{clotri})_2\text{Cl}_2]$ (2) negative scan, (C) $[\text{Co}(\text{clotri})_2\text{Br}_2]$ (6) positive scan, and (D) $[\text{Co}(\text{clotri})_2\text{Br}_2]$ (6) negative scan at 1 mM in CH_3CN with 0.1 M TBAPF₆ as the supporting electrolyte.

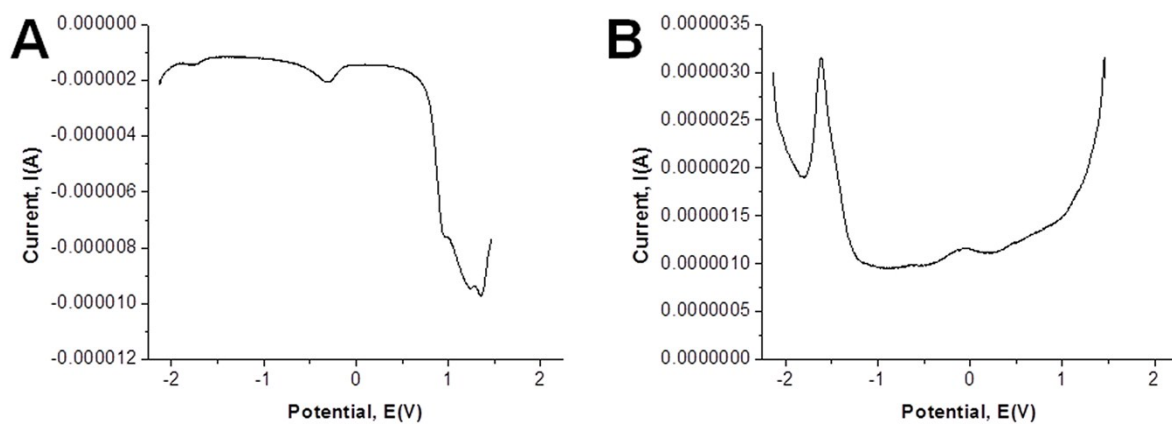


Figure S18. Differential pulse voltammograms vs NHE (A) $[\text{Co}(\text{clotri})_3(\text{NO}_3)_2]$ (**10**) positive scan and (B) $[\text{Co}(\text{clotri})_3(\text{NO}_3)_2]$ (**10**) negative scan at 1 mM in CH_3CN with 0.1 M TBAPF_6 as the supporting electrolyte.

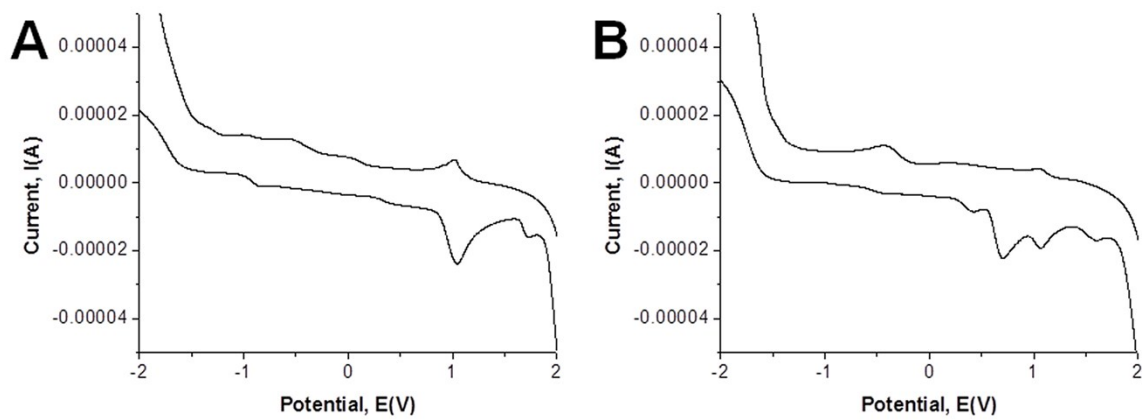


Figure S19. Cyclic voltammograms of A) $[\text{Cu}(\text{clotri})_2\text{Cl}_2] \cdot 5\text{H}_2\text{O}$ (1 mM) and B) $[\text{Cu}(\text{clotri})_2\text{Br}_2] \cdot 5\text{H}_2\text{O}$ (1 mM) in dichloromethane with 0.1 M TBAPF₆ as the supporting electrolyte.